Elliptic anisotropy of open-charm hadrons from parton scatterings in *p*-Pb collisions at energies available at the CERN Large Hadron Collider

Siyu Tang,[1,2] Yuan Lu,[3] Chao Zhang,[4,*] and RenZhuo Wan[2,3,†]

[1] *School of Mathematical and Physical Sciences, Wuhan Textile University, Wuhan 430200, China*
[2] *Hubei Key Laboratory of Digital Textile Equipment, Wuhan Textile University, Wuhan 430200, China*
[3] *School of Electronic and Electrical Engineering, Wuhan Textile University, Wuhan 430200, China*
[4] *School of Science, Wuhan University of Technology, Wuhan 430070, China*

(Received 12 February 2024; revised 9 April 2024; accepted 7 May 2024; published 4 June 2024)

The elliptic azimuthal anisotropy coefficient (v_2) of open-charm hadrons at midrapidity ($|\eta < 1|$) was studied in p-Pb collisions at $\sqrt{s_{NN}} = 8.16$ TeV using a multiphase transport (AMPT) model including an additional charm quark–antiquark pair production trigger. The model provides a simultaneous description of the measured p_{T} spectrum and v_2 of the D^0 meson, as well as the v_2 of light flavor meson K_s^0. We found that the D^0 and K_s^0 v_2 are both significantly affected by different parton scatterings among charm and light quarks. In addition, the predictions for the v_2 of other charm hadrons including D^+, D_s^+, and Λ_c^+ in p-Pb collisions are given for the first time. The v_2 of open-charm hadrons reasonably follows the number-of-constituent-quark (NCQ) scaling up to 2.5 GeV, strongly indicating the importance of partonic degrees of freedom for the collectivity of heavy flavors in high-multiplicity p-Pb collisions. These findings may hint at the formation of deconfined matter in small collision systems, and provide referential value for future measurements of azimuthal anisotropy at energies available at the CERN Large Hadron Collider.

DOI: 10.1103/PhysRevC.109.064902

I. INTRODUCTION

Heavy-ion collisions at ultrarelativistic energies are used to investigate the properties of nuclear matter under extremely high temperatures and energy densities, known as the quark-gluon plasma (QGP) [1,2]. The QGP exhibits the behavior of a nearly perfect fluid, with a low shear viscosity to entropy density ratio [3,4], η/s. The study of the azimuthal anisotropy of final-state particles produced in heavy-ion collisions is a significant approach to constraining the transport properties of the QGP [5,6]. This anisotropy is characterized in terms of the Fourier coefficients $v_n = \langle\cos[n(\varphi - \Psi_n)]\rangle$, where φ is the azimuthal angle of the final-state particle angle and Ψ_n is the symmetry-plane angle in the collision for the nth harmonic [7,8]. The second-order coefficient, v_2, referred to the elliptic flow, is connected to the almond-shaped overlap area formed by colliding nuclei and, as a result, constitutes the primary source of anisotropy in noncentral collisions.

Heavy quarks (charm and beauty) predominantly originate from initial hard-scattering processes characterized by timescales shorter than the QGP formation time, typically around 0.1–1 fm/c, therefore they experience the whole evolution of the QGP, and interact with the constituents of QGP medium [9–11]. Such interactions accompanied by the energy loss lead to a strong modification of the open heavy-flavor hadron (i.e., mesons and baryons that carry one charm or bottom quark/antiquark) yield in heavy-ion collisions with respect to pp collisions, which are widely observed in experiments using the BNL Relativistic Heavy Ion Collider (RHIC) and the CERN Large Hadron Collider (LHC) [12–15]. Further understanding of the interactions of heavy quarks with QGP medium can be gained by analyzing the elliptic flow, v_2, of open heavy-flavor hadrons in heavy-ion collisions. Recent measurements at RHIC [16,17] and LHC [18,19] show that the nonstrange D-meson v_2 at low p_{T} is lower than that of pions and protons, following the the hypothesis of a mass hierarchy. It indicates that the charm quarks participate in the collective expansion of the medium, as well as undergoing recombination with flowing light quarks. Additionally, studying the v_2 of D mesons with strange-quark content (D_s) is also very interesting as it allows further investigation into the effect of charm quark hadronization on D-meson flow [19].

In recent years, the flowlike phenomena of heavy flavors were also observed in small collision systems. The first measurement of elliptic azimuthal anisotropies for prompt D^0 mesons, performed by the CMS Collaboration, indicates that the D^0 v_2 has a sizable value and is lower than light-flavor hadron results [20]. The ALICE Collaboration has measured a significant v_2 of electrons and muons from heavy-flavor hadron decays in p-Pb collisions at mid and forward

*Corresponding author: chaoz@whut.edu.cn
†Corresponding author: wanrz@wtu.edu.cn

rapidities [21–23]. However the origin of such collectivity of heavy flavors in small collision systems is still debated. In hydrodynamics-based models, a sizable v_2 is expected to result from significant interactions between charm quarks and the QGP medium, but it also generates the suppression of particle yield in the high transverse momentum (p_T) region, in contradistinction to the observed unity of $R_{p\mathrm{Pb}}$ for charm hadrons [24–26]. The color-glass condensate (CGC) calculations within the dilute-dense formalism considering the initial-state effect can reproduce the v_2 of nonprompt D mesons well in p-Pb collisions at mid rapidity [27,28], but it overestimates the data at forward rapidity [23]. Recent studies about resolving the R_{pA} and v_2 puzzle of D^0 mesons with the transport models demonstrate the importance of both parton interactions and the Cronin effect in high-multiplicity p-Pb collisions [29].

In addition, an approximate number-of-constituent-quark (NCQ) scaling of v_2 for light flavor hadrons was observed in high-multiplicity p-Pb collisions by the ALICE and CMS Collaborations [20,30]. It triggered discussions about the existence of partonic degree of freedom in small systems. The viscous hydrodynamics combined with the linearized Boltzmann transport (LBT) model, including various hadronization mechanisms, can well describe the identified particle v_2 at intermediate p_T [31]. Our previous studies [32] based on a multiphase transport (AMPT) model demonstrated that the parton scatterings plus quark coalescence can also reproduce the NCQ scaling behavior for light flavor hadrons. However, similar studies were still missing for heavy flavors in p-Pb collisions. Since the charm quarks are proved to be more hydrodynamic than light quarks in final-state azimuthal anisotropy [33], probing the partonic collectivity for heavy quarks is crucial in searching possible formation of the QGP in the small systems at LHC energies.

In this work, we incorporate an additional charm quark-antiquark ($c\bar{c}$) pair trigger in the AMPT model to simultaneously describe the v_2 and p_T spectrum of D^0 mesons in high-multiplicity p-Pb collisions. The first study of the NCQ scaling of v_2 for open-charm hadrons, including D^0, D^+, D_s^+ and Λ_c^+, is performed over the p_T region from 0 to 10 GeV/c. We also investigate how the parton cascade mechanism implemented in AMPT affects elliptic anisotropy of charm hadrons in small collision systems.

II. THE HEAVY-FLAVOR TRIGGERED AMPT MODEL

In this analysis, we employed the string melting version of the AMPT model (v2.26t9b, available online) [34], which has been demonstrated to successfully describe numerous observables at both RHIC and LHC energies. The AMPT is a hybrid framework that includes four main processes: initial conditions, parton scatterings, hadronization, and hadronic rescatterings. The initial conditions are handled by the heavy-ion jet interaction generator (HIJING) two-component model [35], which explicates particle production in the context of both a soft and a hard component. The soft component is modeled by the formation of excited strings in nonperturbative processes, while the hard component involves the production of minijets from hard processes. In these hard processes, hard partons are produced with a momentum transfer larger than the cutoff momentum p_0, to regulates the total minijet production cross section, which can be expressed as

$$\frac{d\sigma^{cd}}{dp_T^2 dy_1 dy_2} = K\sum_{a,b} x_1 f_a(x_1, p_T^2) x_2 f_b(x_2, p_T^2) \frac{d\sigma^{ab\to Q\bar{Q}}}{d\hat{t}}, \tag{1}$$

where y_1 and y_2 represent the rapidities of produced partons, f_a and f_b are the parton distribution functions of parton types a and b in a nucleon, and $\sigma^{ab\to cd}$ is the cross section for partons a and b to produce the minijets c and d. Then the total minijet cross section can be written as

$$\sigma_{\mathrm{jet}} = \sum_{c,d} \frac{1}{1+\delta_{cd}} \int_{p_0^2}^{s/4} dp_T^2 dy_1 dy_2 \frac{d\sigma^{cd}}{dp_T^2 dy_1 dy_2}. \tag{2}$$

The differential cross section of heavy-quark pair in HIJING is evaluated by the perturbative quantum chromodynamics (pQCD) at leading order, which has the same form as Eq. (1):

$$\frac{d\sigma^{Q\bar{Q}}}{dp_T^2 dy_1 dy_2} = K\sum_{a,b} x_1 f_a(x_1, p_T^2) x_2 f_b(x_2, p_T^2) \frac{d\sigma^{ab\to Q\bar{Q}}}{d\hat{t}}, \tag{3}$$

where the same minimum transverse momentum cut p_0 is used in calculating $\sigma^{Q\bar{Q}}$ as done in Eq. (2) for σ_{jet}. However, as described in [36], the heavy quark has large mass, which can naturally regulates the heavy quark total cross section. Therefore, the p_0 cutoff may result in an additional suppression of heavy quark production. For this issue, we employed an approach involving the introduction of a $c\bar{c}$ trigger to significantly enhance the production rate of heavy quarks. This trigger algorithm was initially developed to produce dijet events in the HIJING model [35], then was extended to trigger $c\bar{c}$ pair productions ($q+\bar{q}\to Q+\bar{Q}$, $g+g\to Q+\bar{Q}$). Such an approach was widely used in the study of heavy-flavor hadrons in heavy-ion collisions using the AMPT model [37–39], and it has been demonstrated to be analogous to a recently proposed extended AMPT version [36,39], where the p_0 cutoff was removed for heavy quark production.

In the string melting mechanism, the produced light and heavy quarks are converted into primordial hadrons based on the Lund fragmentation [34]. Two key parameters a and b are used to determine the Lund string fragmentation function as $f(z) \propto z^{-1}(1-z)^a e^{-bm_\perp^2/z}$, where z is the light-cone momentum fraction of the produced hadron of transverse mass $m_\perp$ with respect to the fragmenting string. Then these primordial hadrons are converted into partons according to their flavor and spin structures, thus forming dense partonic matter. The evolution of the partonic matter was simulated using Zhang's parton cascade (ZPC) model [40]. This model incorporates two-body elastic scatterings with a cross section defined by the simplified equation below:

$$\sigma_{gg} \simeq \frac{9\pi\alpha_s^2}{2\mu^2}, \tag{4}$$

where the α_s is the strong coupling constant, and μ is the Debye screening mass. After the partons stop scattering, the nearest two (or three) quarks are combined into mesons (or

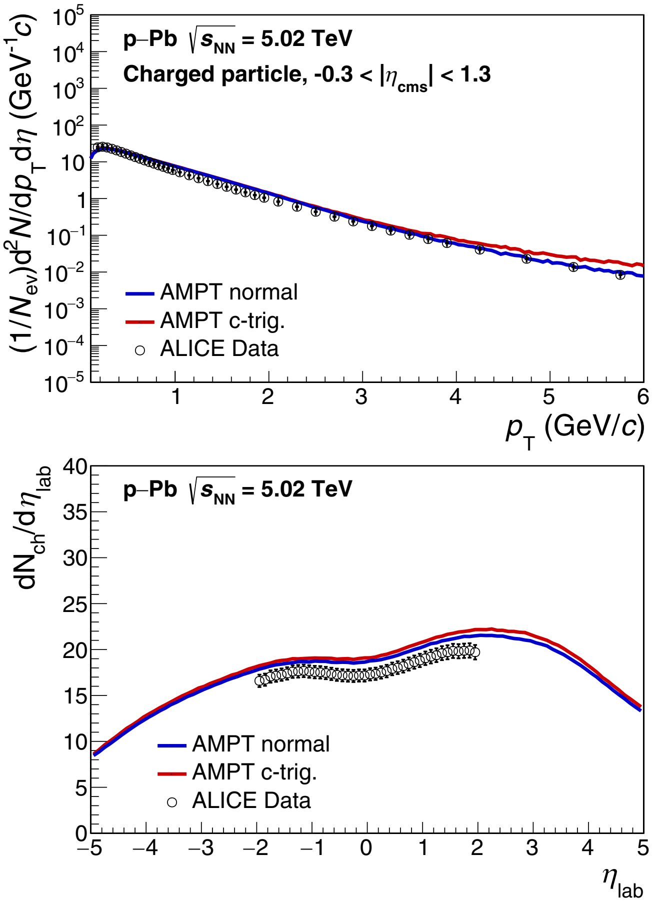

FIG. 1. The p_T spectrum (top) and pseudorapidity density (bottom) of charged particles obtained from the AMPT model are compared to the ALICE measurement [42,43].

baryons) with a quark coalescence model. The subsequent hadronic rescattering processes are described by an extended relativistic transport (ART) model [41] including both elastic and inelastic scatterings for baryon-baryon, baryon-meson, and meson-meson interactions.

In this study, the string melting AMPT models with and without $c\bar{c}$ trigger are used. In both results, 1.2×10^7 events are simulated for inclusive p-Pb collisions at $\sqrt{s_{NN}} = 8.16$ TeV. We set the α_s to 0.33, and adjusted the parton cross section σ ($\sigma = 0, 0.2, 0.5$ mb) by varying the parton screening mass μ. The Lund string fragmentation parameters a and b are set to 0.3 and 0.15 GeV^{-2}, respectively.

III. RESULTS AND DISCUSSIONS

Before studying the elliptic anisotropy of the open-charm hadrons, we test the effect from the charm quark–antiquark pair production trigger on the multiplicity distribution and p_T spectrum of the final-state charged particles. Figure 1 shows the p_T spectrum and the pseudorapidity distribution ($dN_{ch}/d\eta$) of charged particles in p-Pb collisions at $\sqrt{s_{NN}} =$ 5.02 TeV obtained from the AMPT model with and without the additional $c\bar{c}$ trigger, and the comparisons with the ALICE measurement [42,43]. Following the previous studies [29], the parton cascade cross section in the AMPT is set to 0.5 mb. One can see that the results with $c\bar{c}$ trigger (labeled as "AMPT c-trig.") are slightly higher than those without $c\bar{c}$ trigger (labeled as "AMPT normal"), and both sets of calculations provide reasonable descriptions of the data.

Figure 2 shows the p_T spectrum of open-charm mesons (D^0, D^+, D_s) and baryons (Λ_c^+) from the AMPT model with different configurations in p-Pb collisions at $\sqrt{s_{NN}} = 5.02$ TeV in comparison with the ALICE measurement [44,45]. The blue full squares represent the calculations from "AMPT normal", which underestimate all measured charm hadron yields. The results from "AMPT c-trig.", represented by violet full triangles, significantly enhanced the p_T spectrum compared to "AMPT normal", indicating the higher generation rate for the open-charm hadron. Similar phenomena were also observed in previous studies in heavy-ion collisions [38]. From the comparisons with the data shown in Fig. 2, one can see that the calculations from "AMPT c-trig." reasonably describe the measured D^0 yield, but overestimate the D^+ and D_s^+ spectrum. Since the p_T slops of these two AMPT calculations are same, we build two sets of new event samples to describe the D^+ and D_s spectrum with the fractions determined by the data. The green lines shown in Fig. 2 represent the results from such new event samples, with 60% of "AMPT normal" plus 40% of "AMPT c-trig." for D^+, and 40% of "AMPT normal" plus 60% of "AMPT c-trig." for D_s^+. In addition, the data of the Λ_c^+ p_T spectrum are still underestimated by the model calculations even when the $c\bar{c}$ trigger is implemented. This may be ascribed to the coalescence model implemented in the current AMPT version, where the baryons are formed only after the formation of mesons by simply combining three nearest partons regardless of the relative momentum among the coalescing partons [46]. In the following, the two new mixed samples are used to investigate the v_2 of D^+ and D_s^+, and the event sample from "AMPT c-trig." is used for D^0 and Λ_c^+.

In order to directly compare the calculations of v_2 with the data, we exactly follow the two-particle correlation method employed by the CMS experiments [20]. The identified particles within the rapidity range $-1.46 < y_{cm} < 0.54$ are regarded as the trigger particles (denoted as "trig"), then they are correlated with the reference charged particles with $0.3 < p_T < 3$ GeV/c in $-2.4 < \eta < 2.4$ (denoted as "ref"). The azimuthal correlation distribution of these two emission particles can be expanded in the Fourier series as follows:

$$\frac{1}{N_{trig}}\frac{dN^{pair}}{d\Delta\varphi} = \frac{N_{assoc}}{2\pi}\left(1 + 2\sum_{n=1}^{3} V_{n\Delta}(\text{trig, ref})\cos(n\Delta\varphi)\right), \tag{5}$$

where $\Delta\eta$ and $\Delta\varphi$ are the differences in η and φ of each particle pair, $V_{n\Delta}$ are the Fourier coefficients and N_{assoc} represents the total number of pairs per trigger particle. In order to suppress the nonflow contribution from the jet correlations, the $|\Delta\eta| > 1$ is applied in constructing such two-particle correlation. Assuming factorization of the Fourier coefficients, the v_2 of the trigger particles can be obtained by

$$v_2(\text{trig}) = \frac{V_{2\Delta}(\text{trig, ref})}{\sqrt{V_{2\Delta}(\text{ref, ref})}}, \tag{6}$$

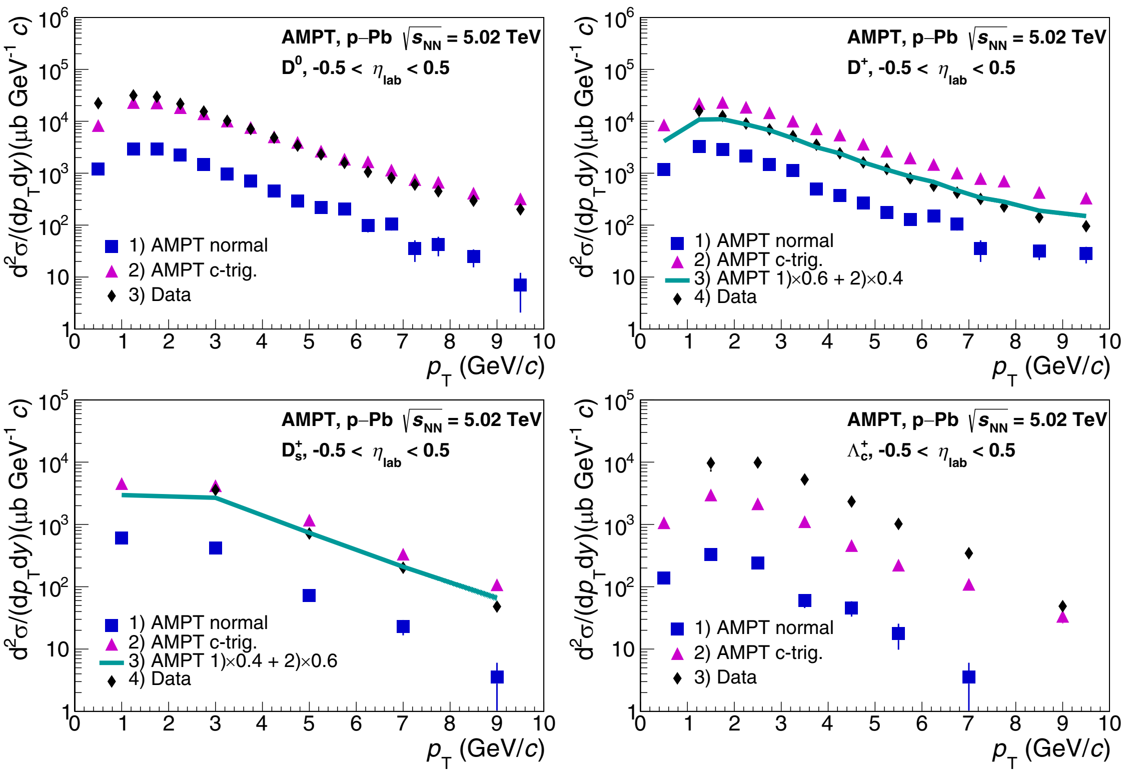

FIG. 2. The cross section of D^0, D^+, D_s^+, and Λ_c^+ as a function of p_T in p-Pb collisions at 5.02 TeV, obtained from AMPT model calculations for different configurations, are compared to the ALICE measurement [44].

Figures 3(a) and 3(b) show the p_T-differential v_2 of D^0 and K_s^0 in p-Pb collisions at 8.16 TeV obtained from the AMPT calculations with the charm-quark trigger, and the comparisons with the CMS data [20]. High multiplicity events within $165 < N_{track} < 250$ are selected,[1] where N_{track} is the number of charged particles with $p_T > 0.4$ GeV/c within $|\eta| < 2.4$. Three sets of parton cross section values are used in the model calculations. One can see that the v_2 of K_s^0 and D^0 have similar p_T trend and magnitude, with the same and nonzero cross section values ($\sigma = 0.2, 0.5$ mb). And both v_2 increase with increasing cross section values. The D^0 v_2 obtained with a parton cross section of 0.2 mb provides a good description of data for $p_T > 3$ GeV/c while the result from 0.5 mb is systematically higher than the data. For K_s^0, the v_2 from 0.5 mb is closer to data compared to other $\sigma = 0.2$ settings. Apparently the calculation with one fixed σ cannot provide a simultaneous description of the v_2 of D^0 and K_s^0. It suggests that the scattering probability among light quarks is higher than that between charm quarks and light quarks, and they may need to be determined from data separately, which was also demonstrated in our previous work [29]. In addition, we

[1]Note that it is a slightly looser selection compared to the cut $185 < N_{track} < 250$ used in the data [20]; however, its effect on v_2 is negligible, as discussed in Fig. 4.

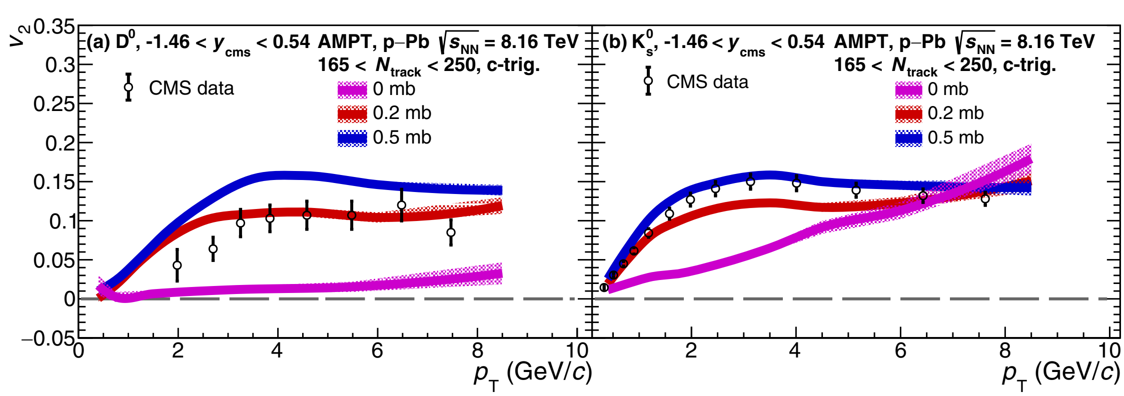

FIG. 3. The v_2 of K_s^0 and D^0 as a function of p_T obtained from the AMPT model calculations with charm quark-anitquark trigger. The results with three set of parton cross section values are shown.

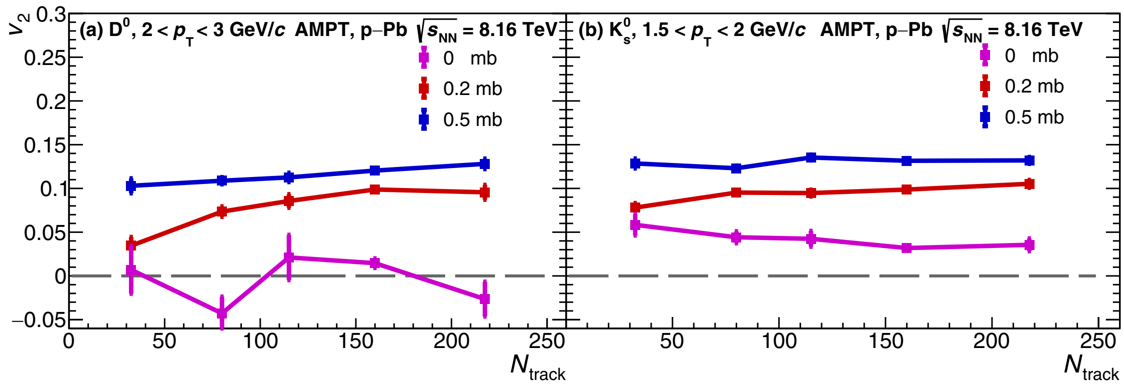

FIG. 4. The v_2 of K_s^0 and D^0 as a function of N_{track} obtained from the AMPT model calculations with charm quark-anitquark trigger. The results with three sets of parton cross section values are shown.

calculate the v_2 of D^0 and K_s^0 when the parton scattering process is turned off ($\sigma = 0$ mb), shown as the dashed lines in Fig. 3. A very small and finite value is obtained for the D^0 v_2, while the K_s^0 v_2 is significant and increases with increasing p_{T}. A similar phenomenon was observed in previous v_2 analysis at the quark level [29]. It indicates that the charm hadron v_2 is mostly generated from the parton scatterings, while for the light flavor hadron, the contribution from the initial state correlation before the parton scattering process (or nonflow) is not negligible especially in the high p_{T} region.

Figures 4(a) and 4(b) present the p_{T}-integrated v_2 of K_s^0 and D^0 as a function of N_{track}. When the implemented cross section value is nonzero ($\sigma = 0.2, 0.5$ mb), the v_2 values slightly increase from low-multiplicity to high-multiplicity events and the same conclusions for $K^{\pm}, \pi^{\pm}$, and protons were obtained in our previous studies [32]. It indicates the larger elliptic anisotropy in more central collisions for both light- and heavy-flavor hadrons, reflecting the changing dynamic conditions and particle production mechanisms in different collision zones. On the other hand, when we exclude the parton scattering process ($\sigma = 0$ mb), the v_2 of K_s^0 decreases with the increasing N_{track}, while the D^0 v_2 fluctuates around 0. It is consistent with our findings about the p_{T}-differential v_2 results in Fig. 3, which hints at a larger nonflow contribution to the v_2 of light quarks in low-multiplicity events compared to charm quarks.

As described above, the nonflow contribution especially from the near-side jet correlation can be suppressed by introducing the pseudorapidity gap ($\Delta\eta > X$) in the two-particle correlation distribution [Eq. (5)]. We vary the $\Delta\eta$ cut in a wide range ($0 < X < 2.4$) and test the stability of v_2 extraction for both D^0 and K_s^0 based on these cuts. To reflect the real data as closely as possible, the parton scattering cross section σ is set to 0.2 mb for D^0, and 0.5 mb for K_s^0. Figure 5 shows the calculated D^0-charged (left) and K_s^0-charged (right) correlation distribution with various cuts ($X = 0.2, 0.6, 1.0, 1.4, 1.8$). One can clearly see that the near-side ($-0.5\pi < \Delta\varphi < 0.5\pi$) correlation distribution is gradually reduced with the increase of the $\Delta\eta$ cut, indicating the subtraction of the near-side jet correlation. Figure 6 (left) shows the p_{T}-differential v_2 for D^0 and K_s^0 with these applied $\Delta\eta$ cuts. With the increase of $\Delta\eta$ cut, the v_2 for both D^0 and K_s^0 decrease, especially in the high p_{T} region where the jet contribution is dominant. In addition, we also investigate the dependence of v_2 on $\Delta\eta$ cut, as shown in Fig. 6 (right). One can see that the v_2 of D^0 and K_s^0 in $5 < p_{\mathrm{T}} < 7$ GeV/c decreases with increasing width of the introduced η gap, but becomes almost flat for $\Delta\eta > 1$. It indicates that the applied $\Delta\eta > 1$ cut is reasonable to suppress the nonflow contribution, and reflects the maximum width of the near-side jet correlation in high-multiplicity p-Pb collisions.

To further investigate the elliptic anisotropy of open-charm hadrons in small collision systems, we extend the calculations

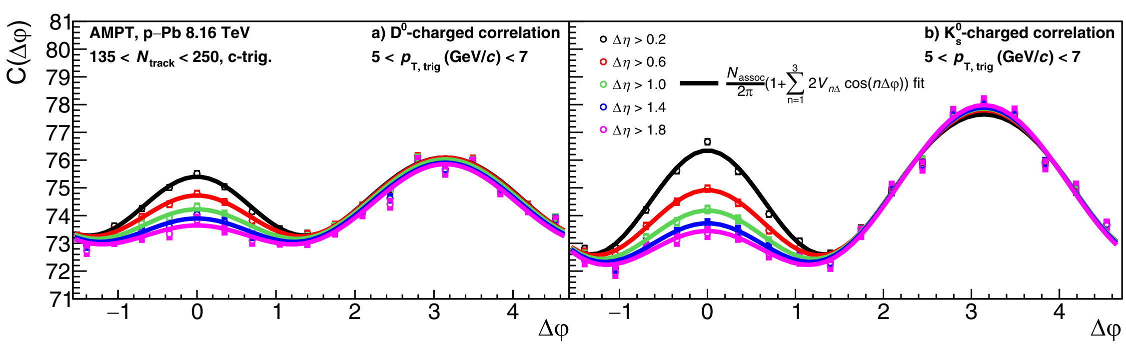

FIG. 5. The distributions for D^0-charged (left) and K_s^0-charged (right) correlation with different $\Delta\eta$ cuts. The trigger particles are selected in $5 < p_{\mathrm{T}} < 7$ GeV/c.

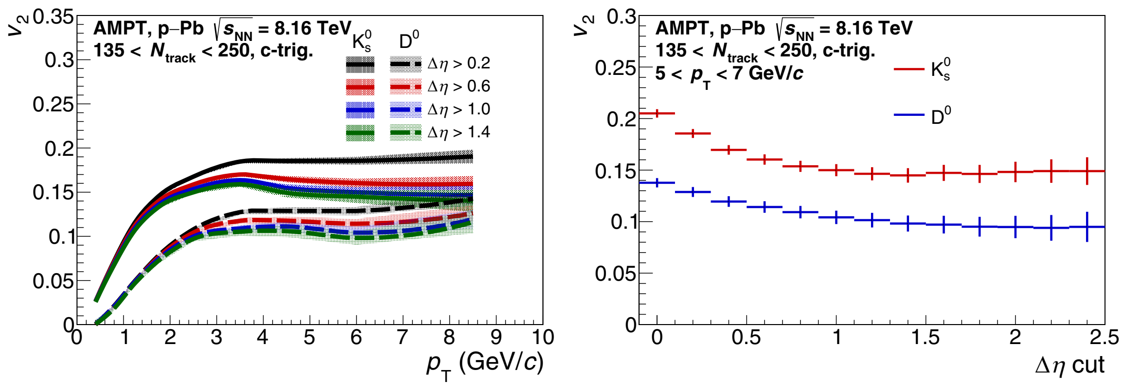

FIG. 6. Left: the v_2 of D^0 and K_s^0 as a function of p_T with various $\Delta\eta$ cuts. Right: the v_2 of D^0 and K_s^0 as a function of $\Delta\eta$ cut.

of v_2 to D_s^+, D^+, and Λ_c^+, as shown in Fig. 7. As discussed above, the AMPT model with charm quark-antiquark trigger is used for the D^0 and Λ_c^+, and mixed event samples introduced in Fig. 2 are used for D^+ and D_s^+. The parton scattering cross section value σ is set to 0.2 mb, which is same as that for D^0. One can see that the v_2 for all charm-hadron species is nonzero. The v_2 of D^0, D^+, and D_s^+ are consistent within uncertainties, which is compatible to the findings in heavy-ion collisions [18]. The v_2 of Λ_c^+ is larger than that of charm mesons for $p_T > 2$ GeV/c, indicating that meson-baryon grouping behaviors are also present in the heavy flavor sector. Future measurements about the elliptic flow of charm baryons can provide more constraints on our calculations.

As discussed in Ref. [47], the observed meson-baryon particle type grouping for flow measurements in heavy-ion collisions indicates the collective behavior at the partonic level, which can be further studied by means of the NCQ scaling technique [48]. In this work, the NCQ scaling behavior of open-charm hadrons in p-Pb collisions is investigated for the first time. Figure 8 presents v_2/n_q as a function of kE_T/n_q for D^0, D^+, D_s^+, and Λ_c^+, and the comparison with the results of light-flavor hadrons including K_s^0, $\pi^\pm$, $K^\pm$ is also shown. Compared to Fig. 7, the v_2 of all particle species is divided by the number of constituent quarks, n_q ($n_q = 2$ for meson, $n_q = 3$ for baryon), and p_T is replaced by the n_q-scaled transverse kinetic energy kE_T/n_q in consideration of the different masses of hadrons, where $kE_T = m_T - m_0 = \sqrt{p_T^2 + m_0^2} - m_0$. We found that all charm hadrons show a set of similar v_2 values after the NCQ scaling, confirming that the quark degree of freedom in flowing matter can also be probed for heavy quarks in the transport model. On the other hand, the v_2 after the NCQ scaling for K_s^0 obtained with the parton scattering cross section $\sigma = 0.5$ mb is compatible with results for $\pi^\pm$ and $K^\pm$, and all of them show a larger value than that of charm hadrons. It suggests that the weaker collective behavior of charm quarks compared to light quarks is mainly attributed to their different parton scatterings.

IV. SUMMARY

In summary, we studied the elliptic anisotropy of open-charm hadrons in p-Pb collisions at $\sqrt{s_{NN}}$ 8.16 TeV by means of introducing an additional charm quark-antiquark pair production trigger in the AMPT model. The implementation of this trigger provides an efficient way to simultaneously describe the p_T spectrum and v_2 of D^0. Then we systematically investigated the dependence of v_2 on parton cross section in various multiplicity ranges, and demonstrate the

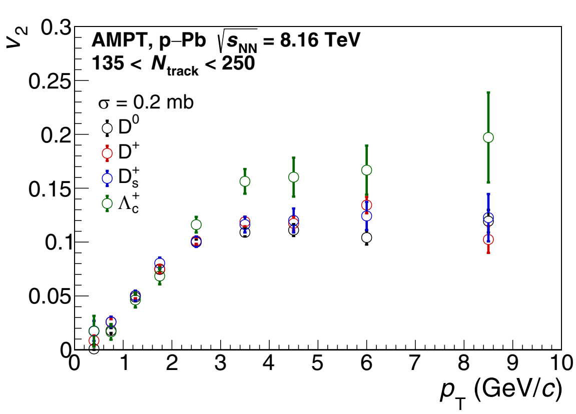

FIG. 7. The v_2 of D^0, D^+, D_s^+, and Λ_c^+ as a function of p_T obtained from the AMPT model calculations with charm quark-anitquark trigger.

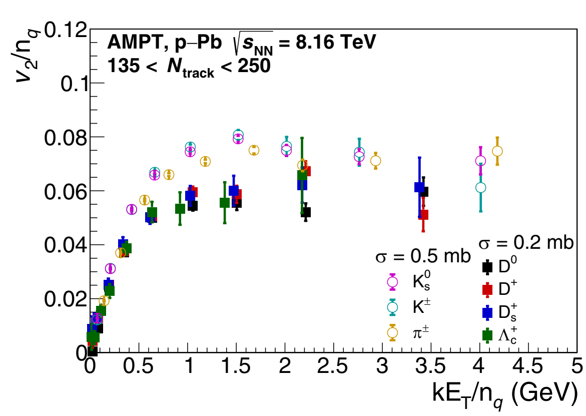

FIG. 8. The kE_T-differential v_2 of D^0, D^+, D_s^+, and Λ_c^+ scaled by the the number of constituent quarks. The comparison to the results of K_s^0, $K^\pm$, and $\pi^\pm$ is also shown.

importance of parton interactions for generating the collectivity of heavy quarks in p-Pb collisions. In addition, we provided new predictions for the v_2 of other charm hadrons including D^+, D_s^+, and Λ_c^+ in p-Pb collisions. We argue that the v_2 of open-charm hadron follows the NCQ scaling in high-multiplicity p-Pb collisions at LHC energies with a proper parton cross section value, indicating the existence of partonic degrees of freedom for heavy quarks in high-multiplicity small collision systems. Future studies about more types of heavy-flavor hadrons, including charmonium and bottom hadrons, can provide further understanding on the transport properties of heavy quarks, and help the search for the possible formation of the hot medium in small systems.

ACKNOWLEDGMENTS

This work was supported by Natural Science Foundation of Hubei Provincial Education Department under Grant No. Q20131603, the Natural Science Foundation of Hubei Province under Grant No. 2024AFB136 and by the Key Laboratory of Quark and Lepton Physics (MOE) in Central China Normal University under Grants No. QLPL2022P01 and No. QLPL202106.

[1] E. V. Shuryak, Phys. Lett. B **78**, 150 (1978).
[2] E. V. Shuryak, Phys. Rep. **61**, 71 (1980).
[3] G.-Y. Qin, H. Petersen, S. A. Bass, and B. Müller, Phys. Rev. C **82**, 064903 (2010).
[4] D. Teaney and L. Yan, Phys. Rev. C **83**, 064904 (2011).
[5] J.-Y. Ollitrault, Phys. Rev. D **46**, 229 (1992).
[6] S. A. Voloshin, Nucl. Phys. A **827**, 377c (2009).
[7] S. Voloshin and Y. Zhang, Z. Phys. C **70**, 665 (1996).
[8] A. M. Poskanzer and S. A. Voloshin, Phys. Rev. C **58**, 1671 (1998).
[9] H. van Hees, V. Greco, and R. Rapp, Phys. Rev. C **73**, 034913 (2006).
[10] N. Brambilla, S. Eidelman, B. K. Heltsley, R. Vogt, G. T. Bodwin, E. Eichten, A. D. Frawley, A. B. Meyer, R. E. Mitchell, V. Papadimitriou *et al.*, Eur. Phys. J. C **71**, 1534 (2011).
[11] A. Andronic, F. Arleo, R. Arnaldi, A. Beraudo, E. Bruna, D. Caffarri, Z. Conesa del Valle, J. G. Contreras, T. Dahms, A. Dainese *et al.*, Eur. Phys. J. C **76**, 107 (2016).
[12] M. Gyulassy and L. McLerran, Nucl. Phys. A **750**, 30 (2005).
[13] J. Adams *et al.* (STAR Collaboration), Nucl. Phys. A **757**, 102 (2005).
[14] K. Adcox *et al.* (PHENIX Collaboration), Nucl. Phys. A **757**, 184 (2005).
[15] B. Müller, J. Schukraft, and B. Wysłouch, Ann. Rev. Nucl. Part. Sci. **62**, 361 (2012).
[16] L. Adamczyk *et al.* (STAR Collaboration), Phys. Rev. Lett. **118**, 212301 (2017).
[17] M. I. Abdulhamid *et al.* (STAR Collaboration), Phys. Lett. B **844**, 138071 (2023).
[18] S. Acharya *et al.* (ALICE Collaboration), Phys. Lett. B **813**, 136054 (2021).
[19] F. Grosa (ALICE Collaboration), EPJ Web Conf. **171**, 18007 (2018).
[20] A. M. Sirunyan *et al.* (CMS Collaboration), Phys. Rev. Lett. **121**, 082301 (2018).
[21] S. Acharya *et al.* (ALICE Collaboration), Phys. Rev. Lett. **122**, 072301 (2019).
[22] J. Adam *et al.* (ALICE Collaboration), Phys. Lett. B **753**, 126 (2016).
[23] S. Acharya *et al.* (ALICE Collaboration), Phys. Lett. B **846**, 137782 (2023).
[24] X. Du and R. Rapp, J. High Energy Phys. 03 (2019) 015.
[25] S. Cao and X.-N. Wang, Rep. Prog. Phys. **84**, 024301 (2021).
[26] Y. Xu, S. Cao, G.-Y. Qin, W. Ke, M. Nahrgang, J. Auvinen, and S. A. Bass, Nucl. Part. Phys. Proc. **276-278**, 225 (2016).
[27] C. Zhang, C. Marquet, G.-Y. Qin, S.-Y. Wei, and B.-W. Xiao, Phys. Rev. Lett. **122**, 172302 (2019).
[28] C. Zhang, C. Marquet, G.-Y. Qin, Y. Shi, L. Wang, S.-Y. Wei, and B.-W. Xiao, Phys. Rev. D **102**, 034010 (2020).
[29] C. Zhang, L. Zheng, S. Shi, and Z.-W. Lin, Phys. Lett. B **846**, 138219 (2023).
[30] B. B. Abelev *et al.* (ALICE Collaboration), Phys. Lett. B **726**, 164 (2013).
[31] W. Zhao, C. M. Ko, Y.-X. Liu, G.-Y. Qin, and H. Song, Phys. Rev. Lett. **125**, 072301 (2020).
[32] S.-Y. Tang, L. Zheng, X.-M. Zhang, and R.-Z. Wan, Nucl. Sci. Tech. **35**, 32 (2024).
[33] H. Li, Z.-W. Lin, and F. Wang, Phys. Rev. C **99**, 044911 (2019).
[34] Z.-W. Lin, C. M. Ko, B.-A. Li, B. Zhang, and S. Pal, Phys. Rev. C **72**, 064901 (2005).
[35] M. Gyulassy and X.-N. Wang, Comput. Phys. Commun. **83**, 307 (1994).
[36] L. Zheng, C. Zhang, S. S. Shi, and Z. W. Lin, Phys. Rev. C **101**, 034905 (2020).
[37] H. Wang, J.-H. Chen, Y.-G. Ma, and S. Zhang, Nucl. Sci. Tech. **30**, 185 (2019).
[38] H. Wang and J.-H. Chen, Nucl. Sci. Tech. **32**, 2 (2021).
[39] H. Wang and J.-H. Chen, Nucl. Sci. Tech. **33**, 15 (2022).
[40] B. Zhang, Comput. Phys. Commun. **109**, 193 (1998).
[41] B.-A. Li and C. M. Ko, Phys. Rev. C **52**, 2037 (1995).
[42] S. Acharya *et al.* (The ALICE Collaboration), J. High Energy Phys. 11 (2018) 013.
[43] B. Abelev *et al.* (ALICE Collaboration), Phys. Rev. Lett. **110**, 032301 (2013).
[44] S. Acharya *et al.* (ALICE Collaboration), J. High Energy Phys. 12 (2019) 092.
[45] S. Acharya *et al.* (ALICE Collaboration), Phys. Rev. C **104**, 054905 (2021).
[46] Y. He and Z.-W. Lin, Phys. Rev. C **96**, 014910 (2017).
[47] S. Afanasiev *et al.* (PHENIX Collaboration), Phys. Rev. Lett. **99**, 052301 (2007).
[48] D. Molnár and S. A. Voloshin, Phys. Rev. Lett. **91**, 092301 (2003).